

Modulated phases and devil's staircases in a layered mean-field version of the ANNNI model

Eduardo Nascimento^(1,2), J. P. de Lima⁽¹⁾, and S. R. Salinas⁽²⁾

(1) Departamento de Física, Universidade Federal do Piauí,
CEP 64049–550, Teresina, PI, Brazil

(2) Instituto de Física, Universidade de São Paulo,
Caixa Postal 66318, CEP 05314-970, São Paulo, SP, Brazil

April 29, 2022

Abstract

We investigate the phase diagram of a spin-1/2 Ising model on a cubic lattice, with competing interactions between nearest and next-nearest neighbors along an axial direction, and fully connected spins on the sites of each perpendicular layer. The problem is formulated in terms of a set of noninteracting Ising chains in a position-dependent field. At low temperatures, as in the standard mean-field version of the Axial-Next-Nearest-Neighbor Ising (ANNNI) model, there are many distinct spatially commensurate phases that spring from a multiphase point of infinitely degenerate ground states. As temperature increases, we confirm the existence of a branching mechanism associated with the onset of higher-order commensurate phases. We check that the ferromagnetic phase undergoes a first-order transition to the modulated phases. Depending on a parameter of competition, the wave number of the striped patterns locks in rational values, giving rise to a devil's staircase. We numerically calculate the Hausdorff dimension D_0 associated with these fractal structures, and show that D_0 increases with temperature but seems to reach a limiting value smaller than $D_0 = 1$.

1 Introduction

The Axial-Next-Nearest-Neighbor Ising (ANNNI) model, which includes competing ferro and antiferromagnetic interactions between pairs of spins along an axial direction, is known to display a spectacularly rich phase diagram, with a host of modulated phases [1][2][3][4]. The ANNNI model is perhaps the simplest lattice statistical model to account for the presence of spatially modulated phases in a large variety of physical systems [5][6].

The energy of the ANNNI model on a simple cubic lattice may be written as

$$\mathcal{H}_{ANNNI} = -\frac{1}{2} \sum_{x,y,z} [J_0 \sigma_{x,y,z} \sigma_{x\pm 1,y\pm 1,z} + J_1 \sigma_{x,y,z} \sigma_{x,y,z\pm 1} + J_2 \sigma_{x,y,z} \sigma_{x,y,z\pm 2}], \quad (1)$$

where the sum is over all lattice sites, and $\sigma_{x,y,z} = \pm 1$ is a spin-1/2 variable at site (x, y, z) . We assume ferromagnetic interactions, $J_0 > 0$, between nearest-neighbor sites on the $x - y$ planes, and competing ferromagnetic, $J_1 > 0$, and antiferromagnetic, $J_2 < 0$, interactions between nearest and next-nearest neighbors along the axial z direction. We then introduce a parameter $p = -J_2/J_1 > 0$ to gauge the strength of the competitions, and look at the $T - p$ phase diagram, where T is the absolute temperature. At zero temperature, with $p < 1/2$, one easily shows that the ground state is a trivial ferromagnet. For $p > 1/2$, however, the ground state displays a peculiar antiferromagnetic structure, which has been called a $\langle 2 \rangle$ phase, with two planes of $+$ spins followed by two planes of $-$ spins, along the z direction. In the special (multiphase) point $p = 1/2$, the ground state becomes infinitely degenerate, with the coexistence of a ferromagnetic phase, the antiphase $\langle 2 \rangle$, associated with a period of 4 lattice spacings along the z direction, and a multiplicity of modulated phases of larger periods [7][8].

Several theoretical approaches have been used to account for the complex $T - p$ phase diagram of the ANNNI model, including careful layer-by-layer mean-field calculations [9][10][11], Monte Carlo simulations [7][12] and analyses of (exact) low-temperature series expansions [7][8]. At finite temperature, all of these calculations indicate the springing from the multiphase point of larger-period modulated phases. In particular, early mean-field calculations by Selke and Duxbury [11], which are in asymptotic agreement with the analysis of the low-temperature series expansions, support the existence of a branching process of ramification that explains the onset of new modulated

phases at higher temperatures. More recent self-consistent [13][14] and Monte Carlo [15] calculations may differ in a number of details, but do confirm the general qualitative features of the $T - p$ phase diagrams.

Taking into account the relevance of the ANNNI model, and some remaining questions about the $T - p$ phase diagram in the region of intermediate temperatures, in special the need of a better characterization of the devil's staircase behavior of the succession of commensurate modulated structures, we decided to revisit this problem and check some points. We then consider the exact formulation of a special ANNNI model, with fully connected spins at each layer, which amounts to solving the original problem in the layer-by-layer mean-field approximation with the addition of spin fluctuations along the axial direction. In other words, we investigate the effects of the introduction of additional fluctuations in the old mean-field calculations. This layered-connected ANNNI model, which we call LC-ANNNI, can also be obtained from the usual ANNNI model Hamiltonian on a hypercubic lattice in the limit of infinite coordination of the spins on each layer. In this limit, we assume a coordination $q_{\perp} \rightarrow \infty$ within each layer, with pair interactions of the form J_0/q_{\perp} , and a fixed value of J_0 . Spin variables on each layer are fully connected, but we preserve the short-range character of the competing interactions (and correlations) along the z direction. The free energy of this special model can be written exactly, leading to equations of state that can be numerically analyzed in great detail.

The layout of this paper is as follows. In Section II we define the LC-ANNNI model, write an exact expression for the free energy, and establish the equations of state, which are amenable to a detailed numerical analysis. Also, we describe the equivalent layer-by-layer mean-field approximation for the analogous ANNNI model. A global $T - p$ phase diagram is obtained in Section III, which also contains some comments on the previous mean-field results. Except for some expected quantitative changes, due to taking into account additional axial fluctuations, we do agree with the mean-field calculations of Selke and Duxbury [11], including the branching process, and the recovery of the asymptotic domain-wall analysis near the multiphase point. We draw some graphs of the main wave number of the modulated structures as a function of p , for fixed values of T , and perform a detailed numerical analysis of the fractal character of these devil's staircases. We obtain numerical values for the Hausdorff dimension $D_0 < 1$ of these fractal structures, and show that D_0 increases with temperature, with a limiting value $D_0 \approx 0.8$, which seems to be a common feature of several problems

represented by area-preserving maps [16], and does support the view that the commensurate modulated structures occupy most of the ordered region of the $T - p$ phase diagram. Some concluding remarks are presented in the final Section.

2 The LC-ANNNI model

The Hamiltonian of the analog of the ANNNI model with fully connected spins at each layer, which we call LC-ANNNI model, is given by a sum of a long-range, mean-field term, \mathcal{H}_{lr} , and a short-range term that includes the axial interactions,

$$\mathcal{H} = \mathcal{H}_{lr} + \mathcal{H}_{sr}, \quad (2)$$

with

$$\mathcal{H}_{lr} = - \sum_{z=1}^N \frac{J_0}{2N^2} \left(\sum_{x,y} \sigma_{x,y,z} \right)^2, \quad (3)$$

and

$$\mathcal{H}_{sr} = - \sum_{x,y,z} [J_1 \sigma_{x,y,z} \sigma_{x,y,z+1} + J_2 \sigma_{x,y,z} \sigma_{x,y,z+2}], \quad (4)$$

where we assume that there are N sites along the sides of a cubic lattice. It should be remarked that \mathcal{H}_{sr} includes the axial short-range interactions, and \mathcal{H}_{lr} represents the long-range, mean-field, ferromagnetic interactions between all pairs of sites on each plane perpendicular to the z direction. We then write the partition function,

$$Z = \sum_{\{\sigma_{x,y,z}\}} \exp \left[\sum_z \frac{\beta J_0}{2N^2} \left(\sum_{x,y} \sigma_{x,y,z} \right)^2 - \beta \mathcal{H}_{sr} \right], \quad (5)$$

where $\beta = 1/k_B T$ and the first sum is over all spin configurations.

Using a set of Gaussian identities,

$$\int_{-\infty}^{+\infty} \exp(-x^2 + 2ax) \frac{dx}{\sqrt{\pi}} = \exp(a^2), \quad (6)$$

and discarding some irrelevant terms, it is straightforward to write the more convenient expression

$$Z = \int dm_1 \cdots \int dm_N \exp(-\beta N^3 \phi), \quad (7)$$

where

$$\phi = \frac{J_0}{2N} \sum_{z=1}^N m_z^2 - \frac{1}{\beta N} \ln Z_I(\{m_z\}), \quad (8)$$

and $Z_I(\{m_z\})$ is the partition function of an Ising chain (with competing interactions) in the presence of site-dependent effective fields, $\{J_0 m_z\}$,

$$Z_I(\{m_z\}) = \sum_{\{\sigma_z\}} \exp \left[\sum_{z=1}^N (\beta J_0 m_z \sigma_z + \beta J_1 \sigma_z \sigma_{z+1} + \beta J_2 \sigma_z \sigma_{z+2}) \right], \quad (9)$$

where $\{\sigma_z = \pm 1\}$, for $z = 1, 2, \dots, N$, is a short-hand notation for the spin variables $\{\sigma_{x,y,z} = \pm 1\}$.

To perform calculations in the ordered regions of the phase diagram, it is convenient to use a transfer matrix technique and write

$$\phi = \frac{J_0}{2N} \sum_{z=1}^N m_z^2 - \frac{1}{\beta N} \ln \left(\text{Tr} \prod_{z=1}^N \mathbf{V}_z \right), \quad (10)$$

where the 4×4 matrix \mathbf{V}_z is given by

$$\begin{aligned} \mathbf{V}_z &= \begin{pmatrix} y_z & 0 & 0 & 0 \\ 0 & y_z & 0 & 0 \\ 0 & 0 & y_z^{-1} & 0 \\ 0 & 0 & 0 & y_z^{-1} \end{pmatrix} \\ &\times \begin{pmatrix} x_1 x_2 & x_2^{-1} & 0 & 0 \\ 0 & 0 & x_2^{-1} & x_1^{-1} x_2 \\ 0 & 0 & x_1 x_2 & x_2^{-1} \\ x_2^{-1} & x_1^{-1} x_2 & 0 & 0 \end{pmatrix}, \end{aligned} \quad (11)$$

with

$$x_1 = \exp(\beta J_1), \quad x_2 = \exp(\beta J_2), \quad y_z = \exp(\beta J_0 m_z). \quad (12)$$

In the thermodynamic limit, $N \rightarrow \infty$, the asymptotic form of the partition function comes from an application of Laplace's method.

Given a commensurate phase, the magnetization profile is repeated after a certain finite number n of layers. Therefore, without any loss of generality,

we consider $N = nM$ in Eq. (10). In the thermodynamic limit, we then write the free energy functional

$$\phi = \frac{J_0}{2n} \sum_{z=1}^n m_z^2 - \frac{1}{\beta n} \ln \lambda_0, \quad (13)$$

where λ_0 is the maximum eigenvalue of the matrix

$$\mathbf{V} = \prod_{z=1}^n \mathbf{V}_z. \quad (14)$$

The equilibrium magnetization pattern, $\{m_z\}$, comes from the stationary conditions, $\partial\phi/\partial m_z = 0$, which lead to a set of nonlinear coupled equations,

$$m_z = \frac{\langle l_0 | \mathbf{V}_1 \mathbf{V}_2 \cdots \mathbf{V}_{z-1} \mathbf{S} \mathbf{V}_z \mathbf{V}_{z+1} \cdots \mathbf{V}_n | r_0 \rangle}{\lambda_0 \langle l_0 | r_0 \rangle}, \quad (15)$$

where $|r_0\rangle$ and $|l_0\rangle$ are the right and left eigenvectors of the transfer matrix \mathbf{V} , corresponding to λ_0 , and the matrix \mathbf{S} is given by

$$\mathbf{S} = \begin{pmatrix} 1 & 0 & 0 & 0 \\ 0 & 1 & 0 & 0 \\ 0 & 0 & -1 & 0 \\ 0 & 0 & 0 & -1 \end{pmatrix}. \quad (16)$$

At fixed values of T and p , the stable magnetization profile comes from the solution of Eq. (15) that minimizes the free energy functional ϕ , given by Eq. (13).

2.1 Equivalent mean-field approximation

Consider the Hamiltonian of the ANNNI model on a cubic lattice, given by Eq. (1). A mean-field solution for this problem can be obtained from the variational inequality

$$G(\mathcal{H}) \leq G_0(\mathcal{H}_0) + \langle \mathcal{H} - \mathcal{H}_0 \rangle_0 = \Phi, \quad (17)$$

where $G(\mathcal{H})$ is the free energy of the system, $G_0(\mathcal{H}_0)$ is the free energy of a system associated with a trial Hamiltonian \mathcal{H}_0 , and $\langle \dots \rangle_0$ is an average value

with respect to \mathcal{H}_0 . In the usual layer-by-layer mean-field calculations [10], we use a free trial Hamiltonian,

$$\mathcal{H}_0 = - \sum_{x,y,z} \eta_z \sigma_{x,y,z}, \quad (18)$$

where $\{\eta_z\}$ is a set of field (variational) parameters. It is easy to write $\Phi = \Phi(\{\eta_z\})$, and obtain the mean-field solutions by minimizing this expression of Φ with respect to the field parameters.

In order to include fluctuations along the z direction, we consider another trial Hamiltonian,

$$\mathcal{H}_{01} = -\frac{1}{2} \sum_{x,y,z} [J_1 \sigma_{x,y,z} \sigma_{x,y,z\pm 1} + J_2 \sigma_{x,y,z} \sigma_{x,y,z\pm 2}] - \sum_{x,y,z} \eta_z \sigma_{x,y,z}, \quad (19)$$

which corresponds to independent Ising chains along the z direction. For a cubic lattice, with $N \times N \times N$ sites, it is easy to show that

$$G_{01} = -\frac{N^2}{\beta} \ln Z_{01}, \quad (20)$$

with

$$Z_{01} = \sum_{\{\sigma_z\}} \exp \left[\sum_{z=1}^N [\beta J_1 \sigma_z \sigma_{z+1} + \beta J_2 \sigma_z \sigma_{z+2}] + \sum_{z=1}^N \beta \eta_z \sigma_z \right], \quad (21)$$

where σ_z is a short-hand notation for $\sigma_{x,y,z}$. We then have

$$\Phi = -\frac{1}{\beta} N^2 \ln Z_{01} - N^2 \sum_{z=1}^N J_0 m_z^2 + N^2 \sum_{z=1}^N \eta_z m_z, \quad (22)$$

where

$$m_z = \langle \sigma_{x,y,z} \rangle_0 = \frac{1}{\beta} \frac{\partial}{\partial \eta_z} \ln Z_{01}. \quad (23)$$

Note that m_z depends on the set of field variables $\{\eta_z\}$. In other words, $m_z = m_z(\{\eta_z\})$. The minimization of Φ leads to the condition $\eta_z = J_0 m_z$, which should be inserted into Eq. (23) to produce a set of self-consistent equations for $\{m_z\}$. With the trivial correspondence $J_0 \rightarrow J_0/4$ to account for the four-coordination of the spins on the $x-y$ planes, these expressions lead to the same results already obtained in this Section for the LC-ANNNI model.

3 Analysis of the numerical results

3.1 Paramagnetic critical lines

It is easy to obtain an expression for the transition lines separating the paramagnetic and the ordered phases. Consider an expansion of ϕ , given by Eq. (8), in terms of the effective magnetizations,

$$\phi = \frac{J_0}{2N} \sum_{z=1}^N m_z^2 - \frac{\beta J_0^2}{2N} \sum_{z,z'} \langle \sigma_z \sigma_{z'} \rangle_0 m_z m_{z'} + \dots, \quad (24)$$

where $\langle \sigma_z \sigma_{z'} \rangle_0$ is a zero-field pair correlation of an Ising chain,

$$\langle \sigma_z \sigma_{z'} \rangle_0 = \frac{1}{Z_I(\{0\})} \sum_{\{\sigma_z\}} \sigma_z \sigma_{z'} \exp \left[\sum_{z=1}^N (\beta J_1 \sigma_z \sigma_{z+1} + \beta J_2 \sigma_z \sigma_{z+2}) \right], \quad (25)$$

which has been calculated by Stephenson [17].

The paramagnetic transition lines come from

$$1 = \beta J_0 \chi_0(q_{\max}), \quad (26)$$

where

$$\chi_0(q) = \sum_h \langle \sigma_z \sigma_{z+h} \rangle_0 \exp(-iqh) = \frac{A + B \cos q}{C + D \cos q + E \cos^2 q}, \quad (27)$$

and the coefficients A to E are real functions of βJ_1 and βJ_2 , which have been explicitly obtained by Stephenson [18][19]. We can use these expressions, with $J_0 = 4J_1 = 4J > 0$, to draw the paramagnetic lines, given by Eq. (26), and to locate the Lifshitz point in a phase diagram in terms of $k_B T/J$ and the parameter p , and then compare with the well-known results from the old layer-by-layer mean-field approximations. Due to the inclusion of extra fluctuations along the axial direction, it is not surprising that the critical temperature is slightly smaller than the old mean-field values. Similar results had already been obtained in previous calculations for the ANNNI model, which were, however, limited to the analysis of the paramagnetic border [20][19].

3.2 Phase diagrams

The mean-field equations (15) were solved numerically using quadruple precision. All integer values of n should be considered to obtain the modulated structures that minimize the free energy functional (13). However, since this is not feasible, earlier calculations were limited to a relatively small set of modulated phases (with $n \lesssim 20$) [9][10]. A real advance in these calculations has been achieved by Selke and Duxbury [11][2], with the proposal of a structure combination branching mechanism to explain the onset of different commensurate phases at increasing temperatures. According to this mechanism, at $T > 0$, the boundaries between two adjacent modulated phases, which we call A and B , will become unstable against a new intervening phase AB . For example, using the standard notation for the modulated phases of the ANNNI model [2], consider the ordered structures (i) $A = \langle 3 \rangle$, which consists of three planes of (predominantly) $+$ spins followed by three planes of $-$ spins, in a periodic pattern along the axial direction, and (ii) $B = \langle 32 \rangle$, which consists of three planes of $+$ spins, followed by two planes of $-$ spins. These phases will become unstable against the new intervening phase $AB = \langle 332 \rangle$. In more general terms, given the phases $A = \langle 32^{j-1} \rangle$ and $B = \langle 32^j \rangle$, with $j = 1, 2, 3, \dots$, we have the new intervening phase $AB = \langle 32^{j-1}32^j \rangle$.

In Fig. 1, we show the main commensurate structures in the $T - p$ phase diagram, with $J_0 = J_1 = J > 0$, and $p = -J_2/J$. We have four large regions: paramagnetic, ferromagnetic (ferro), the antiphase $\langle 2 \rangle$, and the large region of modulated structures. According to the expectations, the paramagnetic critical border meets tangentially the first-order ferro-modulated border at the Lifshitz point (LP). As the temperature increases, we checked that long-period structures become stable in smaller regions of this phase diagram. We recall that the notation $\langle 3 \rangle$ means that there are 3 planes of $+$ spins followed by 3 planes of $-$ spins along the axial direction. Although we use a different temperature scale, the general qualitative topology of this phase diagram is the same as obtained in the earlier mean-field calculations. Modulated phases $\langle 2 \rangle$, $\langle 3 \rangle$, $\langle 4 \rangle$, and $\langle 32 \rangle$ still occupy large portions of the modulated region.

In the vicinity of the multiphase point, both the LC-ANNNI and the standard ANNNI model display the same qualitative features. Simple periodic structures of the type $\langle 32^j \rangle$ still play a major role at low temperatures. In addition, the $\langle 4 \rangle$ phase displays a range of stability between $\langle \infty \rangle$ and $\langle 3 \rangle$. This behavior is consistent with the predictions of the domain-wall analysis

for sufficiently anisotropic cases [8].

In all of our calculations, we have fully confirmed the branching mechanism, which keeps working in the modulated regions, as the temperature increases, and helps to drastically reduce the number of phases to be analyzed. The wave number of the new modulated phase is in the interval between the wave numbers of the parent modulated phases, according to the rule for the construction of a Farey tree. As the temperature increases, the wave numbers of the new modulated phases, in units of 2π , will tend to cover all the rational numbers.

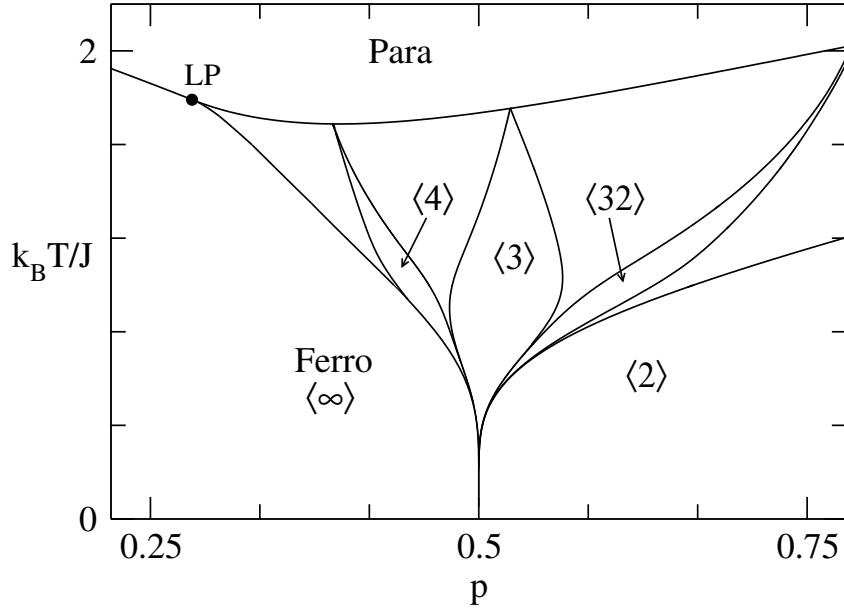


Figure 1: Main commensurate phases in the global $T - p$ phase diagram of the LC-ANNNI model (with $J_0 = J_1 = J > 0$, $p = -J_2/J_1 > 0$). The paramagnetic border comes from Eq.(26). The Lifshitz point is located at $p_{LP} = 0.28172\dots$ and $k_B T_{LP}/J = 1.79152\dots$

In Fig.2, we draw a typical graph of the wave number of modulated phases versus temperature for a particular value of the parameter of competition, $p = 0.57$ (and with $J_0 = J_1 = J > 0$). We have used the branching mechanism, with quadruple precision, to draw this graph (and the graphs of the following figures). The simple periodic structures are associated with

wide plateaus of stability, and there are higher-order commensurate phases between the main commensurate structures.

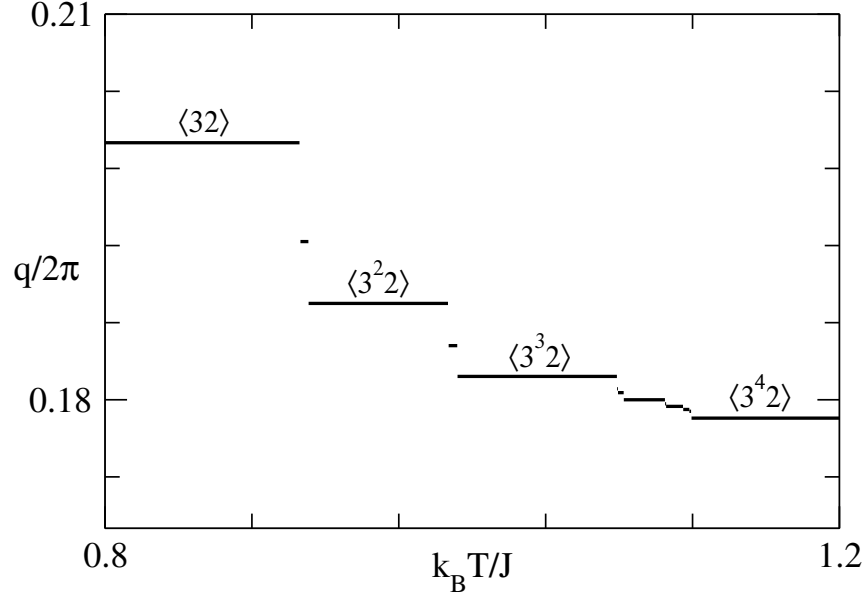


Figure 2: Typical graph of the wave number of the main modulated phases versus temperature for $p = 0.57$ (with $J_0 = J_1 = J > 0$). Note the existence of higher-order commensurate phases in the intervals between the plateaus.

In the immediate vicinity of the Lifshitz point, we can analytically show that the ferro-modulated border is discontinuous. In order to further check the nature of this border, in Fig. 3 we draw a graph of the main wave number of the modulated structures as a function of p , for fixed temperature $k_B T/J = 1.1$ (with $J_0 = J_1 = J > 0$). We indicate the modulated phases associated with the largest plateaus, $\langle 3 \rangle$, $\langle 43 \rangle$, and $\langle 4 \rangle$, and draw this graph to point out the discontinuous character of the transition to the ferromagnetic phase ($q = 0$), which does agree with the old mean-field and domain-wall calculations (and disagrees with the variational calculations of Gendiar and Nishino [14]).

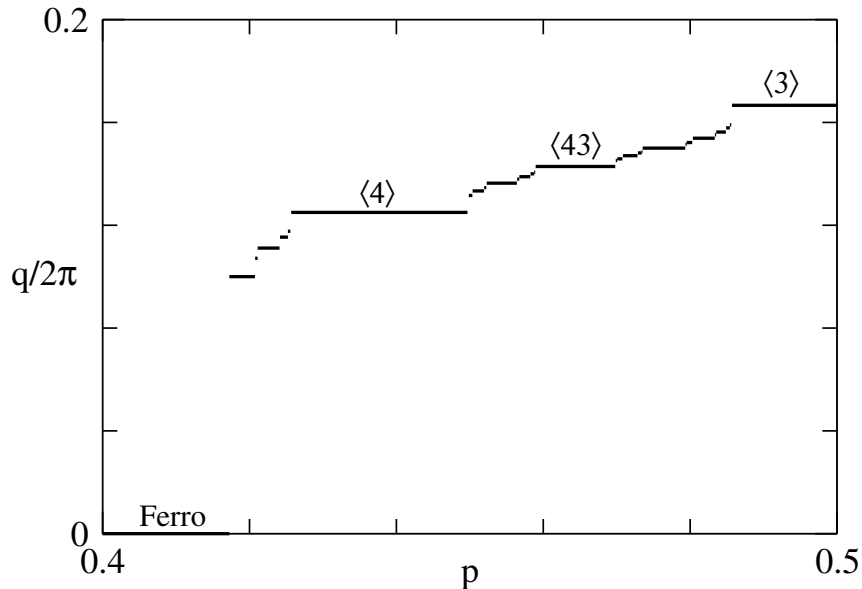


Figure 3: Graph of the main wave number of the modulated structures as a function of p , for fixed temperature $k_B T/J = 1.1$ (with $J_0 = J_1 = J > 0$).

3.3 Devil's staircases

At fixed temperature, as we change the parameter p , the wave number locks in rational values, which gives rise to a sequence of phase transitions. At intermediate temperatures, many distinct commensurate phases are locked in finite regions of stability. For example, the simple periodic phases $\langle 3^n 2 \rangle$ and $\langle 32^n \rangle$ lock in large intervals of the parameter p (see Fig. 4). These results are in quantitative disagreement with the claims of some recent Monte Carlo simulations for the ANNNI model, which seem to support much narrower ranges of stability of the modulated structures [15]. In contrast, phases $\langle 3 \rangle$ and $\langle 32 \rangle$ are shown to occupy small regions in the phase diagram, as it has been obtained in these Monte Carlo simulations.

We now turn to the question of the fractal dimension of the q versus p graphs. We use a well-known box-counting algorithm to estimate the fractal dimension of the set of points that remain in an interval of values of q if we subtract all of the intervals corresponding to plateaux of the commensurate phases larger than a certain (limiting small) width. For example, consider the plateaux in the graph of q versus p of Fig. 4, and look at the interval

between $q_i = 0.5$ and $q_f = 0.8$. Calculate the difference $X(\epsilon)$ between the width $q_f - q_i$ and the sum of the intervals corresponding to the commensurate phases with plateaux of widths larger than a certain length $\epsilon > 0$. The slope of a log-log plot of $X(\epsilon)/\epsilon$ versus $1/\epsilon$, in the limit of small values of ϵ , gives the Hausdorff fractal dimension D_0 associated with the (much smaller) plateaux of the remaining set of phases. If $D_0 < 1$, the remaining (presumably incommensurate) phases occupy a fractal set (of zero measure). This is the anticipated situation at intermediate temperatures, at least not so close to the paramagnetic transition. If $D_0 < 1$, we say that we have a complete devil's staircase.

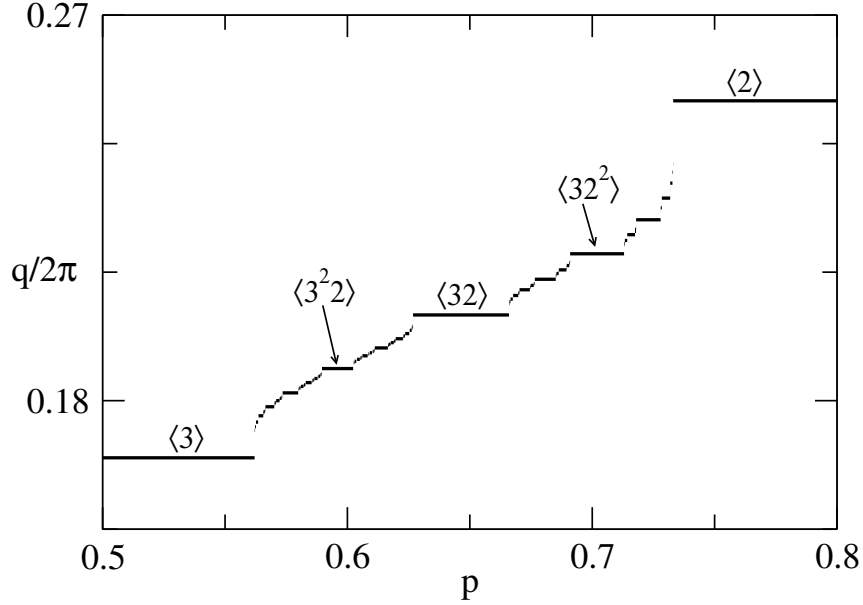


Figure 4: Wave number versus p for $k_B T/J = 1.125$. There is a cascade of phase transitions as the wave number q goes from $2\pi/6$ (in the $\langle 3 \rangle$ phase) to $2\pi/4$ (in the $\langle 2 \rangle$ phase). Many distinct commensurate modulated phases are stable. We show phases associated with plateaux of width $\Delta p > 10^{-5}$ only.

In Fig. 5, we show numerically obtained plots of $\log[X(\epsilon)/\epsilon]$ versus $\log[1/\epsilon]$ for $k_B T/J = 1.1$ (graph A) and $k_B T/J = 1.15$ (graph B). From these straight lines, we obtain the Hausdorff dimensions, which are plotted in Fig. 6, for a few increasing values of temperature, below the paramagnetic critical line. As $D_0 < 1$, we have complete devil's staircases (in other words,

at these temperatures, incommensurate phases occupy a region of fractal measure). Since these calculations are much harder at higher temperatures, we can only claim that we have numerical evidence that $D_0 < 1$ increases with temperature, and seems to reach a value smaller than $D_0 \approx 0.8$, which is in agreement with numerical calculations for several mapping problems [16].

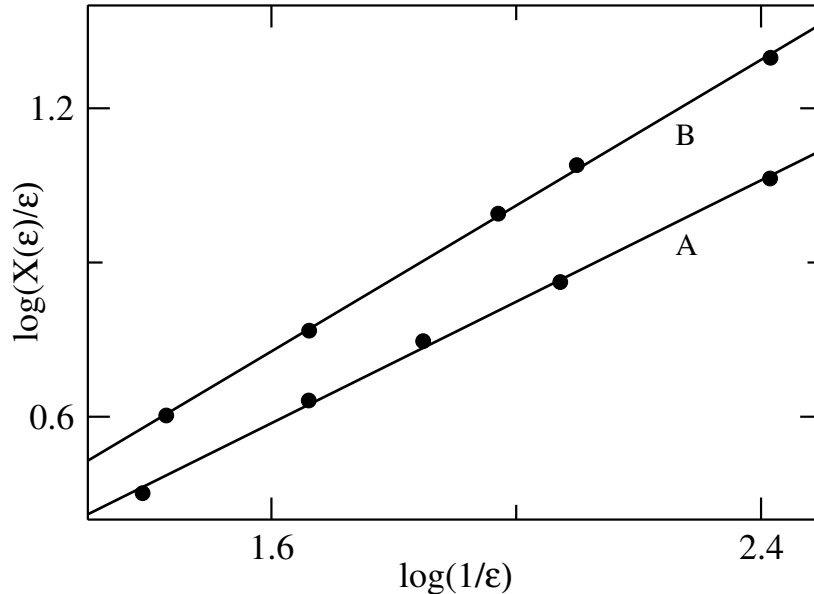


Figure 5: Plots of $\log [X(\epsilon)/\epsilon]$ versus $\log [1/\epsilon]$ for $k_B T/J = 1.1$ (graph A) and $k_B T/J = 1.15$ (graph B).

4 Conclusions

We investigated the equilibrium behavior of a spin-1/2 Ising system with axial competing interactions between nearest and next-nearest neighbors, and infinite-range interactions between spins on the sites of planes perpendicular to the axial direction. This system may be regarded as obtained from a particular limit of infinite coordination of the layers of the ANNNI model on a hypercubic lattice. The same results can also be obtained from a mean-field variational treatment of the ANNNI model on a hypercubic lattice [10],

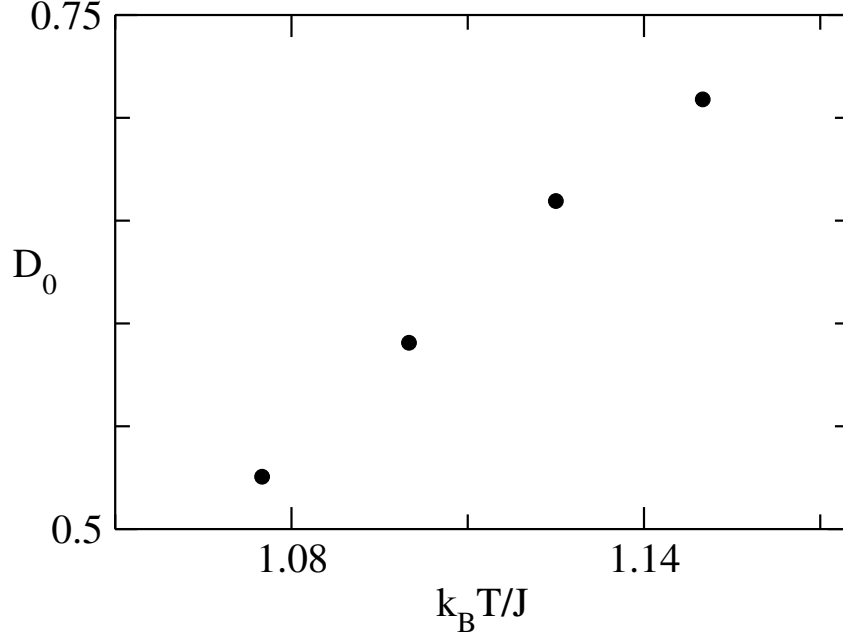


Figure 6: Hausdorff fractal dimension D_0 as function of temperature ($k_B T/J$, with $J_0 = J$). Note that $D_0 < 1$ increases with temperature.

if we use a trial Hamiltonian formed by set of independent Ising chains, with next-nearest-neighbor interactions, in a position-dependent field.

On the basis of an expression for the free energy, we perform numerical calculations to check the main features of the phase diagram and the main spatially modulated phases. At low temperatures, in accordance with the domain-wall analysis of the ANNNI model, the ferromagnetic and the $\langle 2 \rangle$ phases melt via a first-order transition into the modulated phases. At quite low temperatures, the $\langle 4 \rangle$ phase has a small range of stability, between the ferromagnetic and $\langle 3 \rangle$ phases, which depends upon the model parameters. Higher-order commensurate phases become stable with increasing temperatures. We confirm the existence of a branching mechanism to stabilize long-period modulated structures at increasing temperatures (note that we are assuming $J_0 = J_1$). In terms of either temperature or the parameter of competition, the main wave number of the modulated phases divided by 2π locks at rational values. We draw some graphs of these wave numbers as a

function of p , for fixed values of T , and perform a detailed numerical analysis of the fractal character of the associated devil's staircases. We calculate the Hausdorff dimension $D_0 < 1$ of these fractal structures, and show that D_0 increases with temperature, with a limiting value $D_0 \approx 0.8$, which seems to be a common feature of several problems represented by area-preserving maps. We support the picture that simple periodic phases play the main role in the ordered region of the $T - p$ phase diagram.

References

- [1] Per Bak, Repts. Progr. Phys. **45**, 587, 1988.
- [2] W. Selke, Phys. Repts. **170**, 213, 1988.
- [3] Julia Yeomans, Solid State Physics **41**, 151, 1988.
- [4] W. Selke, in Phase Transitions and Critical Phenomena, vol. 15, edited by C. Domb and J. L. Lebowitz, Academic Press, London, 1992.
- [5] K. Owada, Y. Fujii, J. Murakoa, H. Nakao, Y. Murakami, Y. Noda, H. Ohsumi, N. Ikeda, T. Shobu, M. Isobe, and Y. Ueda, Phys. Rev. B **76**, 094113, 2007.
- [6] O. Ouisse and D. Chaussende, Phys. Rev. B **85**, 104110, 2012.
- [7] W. Selke and M. E. Fisher, Phys. Rev. B **20**, 257, 1979; M. E. Fisher and W. Selke, Phys. Rev. Lett. **44**, 1502, 1980; M. E. Fisher and W. Selke, Phil. Trans. R. Soc. London **302**, 1, 1981.
- [8] A. M. Szpilka and M. E. Fisher, Phys. Rev. Lett. **57**, 1044, 1986; M. E. Fisher and A. M. Szpilka, Phys. Rev. B **36**, 5343, 1987.
- [9] P. Bak and J. von Boehm, Phys. Rev. B **21**, 5297, 1980.
- [10] C. S. O. Yokoi, M. D. Coutinho-Filho and S. R. Salinas, Phys. Rev. B **24**, 4047, 1981.
- [11] W. Selke and P. M. Duxbury, Z. Phys. B **57**, 49, 1984.
- [12] K. Kaski and W. Selke, Phys. Rev. B **31**, 3128, 1985.

- [13] A. Surda, Phys. Rev. B **69**, 134116, 2004.
- [14] A. Gendiar and T. Nishino, Phys. Rev. B **71**, 024404, 2005.
- [15] K. Zhang and P. Charbonneau, Phys. Rev. Lett. **104**, 195703, 2010; K. Zhang and P. Charbonneau, Phys. Rev. B **83**, 214303, 2011.
- [16] O. Biham and D. Mukamel, Phys. Rev. A **39**, 5326, 1989.
- [17] J. Stephenson, Can. J. Phys. **48**, 1724, 1970.
- [18] J. Stephenson, Phys. Rev. B **15**, 5442, 1977.
- [19] I. Harada, J. Phys. Soc. Japan **52**, 4099, 1983.
- [20] A. S. T. Pires, N. P. Silva, and B. J. O. Franco, Phys. Stat. Sol. (b) **114**, K63, 1982.